PFC/JA-84-21

LOWER HYBRID WAVE PROPAGATION IN TOROIDAL PLASMAS

J. J. Schuss[†]

Plasma Fusion Center
Massachusetts Institute of Technology
Cambridge, MA 02139

June 1984

This work was supported by the U.S. Department of Energy Contract No. DE-AC02-78ET51013. Reproduction, translation, publication, use and disposal, in whole or in part by or for the United States government is permitted.

By acceptance of this article, the publisher and/or recipient acknowledges the U.S. Government's right to retain a non-exclusive, royalty-free license in and to any copyright covering this paper.

[†] Present address: Raytheon Co., Wayland, Massachusetts 01778

Lower Hybrid Wave Propagation

in Toroidal Plasmas

J. J. Schuss*
Plasma Fusion Center
Massachusetts Institute of Technology
Cambridge, Mass. 02139

Abstract

The electrostatic lower hybrid wave equation is solved in toroidal geometry by expanding the wave potential as a sum of poloidal eigenmodes and calculating their mutual coupling to first order in $\varepsilon = r/R$. The resulting solutions are compared to toroidal ray tracing calculations. These solutions present a technique that can explicitly determine the evolution of the wave poloidal mode number spectrum over long trajectories that involve multiple passes of the plasma column.

* Present Address: Raytheon Company, Wayland, Mass. 01778

There is presently active interest in the use of lower hybrid waves in tokamaks for driving toroidal plasma currents and also for electron heating. These rf driven plasma currents can be sustained in the absence of an externally applied loop voltage and could be employed to yield steady state tokamak operation. Lower hybrid wave injection has been used to enhance the external transformer driven plasma current in the JFT-2, WT-2, Versator II, and the JIPP T-II [1-4] tokamaks, and to maintain the plasma current in the absence of an externally driven loop voltage in the PLT[5] and Alcator C[6,7] tokamaks. Recently, lower hybrid wave injection has been used to initiate and maintain a low density ($\bar{n}_e \sim 10^{12}$ cm^{-3}) plasma discharge in PLT[8].

A complication of the lower hybrid wave-plasma interaction is the absence of a well defined resonance that causes the plasma electrons to absorb the wave energy on the wave's first pass of the plasma column. In addition, the value of $k_\parallel = \vec{k}\cdot\vec{B}/|\vec{B}|$ varies as the wave propagates into the plasma due to toroidal effects. The strength of the wave-electron interaction in an initially Maxwellian plasma is exponentially dependent on this same $k_\parallel$. The evolution of the lower hybrid wave as it propagates through the plasma has been studied using ray tracing, both for multiple passes of the plasma[9] and for a single pass[10]. Due to the toroidal downshift of $k_\parallel$ on the wave's first pass when it is launched from the low field side of the torus, it must usually execute several loops through the plasma before it is damped out.

These ray tracing calculations ignore any broadening in the wave's poloidal mode number m spectrum as the wave propagates through the plasma. Electron Landau damping and current drive are dependent on the $k_\parallel$

spectrum, which depends on m as

$$k_{\parallel} = m/r \sin\delta + k_{\phi} \cos\delta \qquad (1)$$

Here $\tan\delta = B_{\theta} / B\phi$, where B_{θ} is the poloidal field, $B\phi$ is the local toroidal field, and $n = Rk_{\phi}$ is the toroidal mode number, (i.e., all fields vary as $\exp(in\phi)$ where n a constant and ϕ is the toroidal angle). The strong dependence of wave damping on $k_{\parallel}$ and therefore on m can distort the wave's m spectrum. It should also be noted that the finite poloidal extent of the waveguide launching structure results in the wave being characterized by both a spatial and an m spectral width that need to be taken into account in wave propagation.

For these reasons there is a need to formulate a full wave solution to the lower hybrid wave equation in toroidal geometry. A solution to the electrostatic wave equation has been pursued using a ballooning mode formalism.[11,12] In this paper a straightforward method of solution to this wave equation is presented using an expansion of the wave in poloidal eigenmodes. This method is employed to generate solutions to the lower hybrid wave equation in plasmas having similar parameters to those of Alcator C. While the cases presented here are simple and ignore wave absorption, this method can be expanded to handle more complex wave heating scenarios.

In this method the electric field $\bar{E} = - \nabla\Phi(r,\theta,\phi)$, where we expand

$$\Phi(r,\theta,\phi) = \sum_{m} \Phi_{m}(r) e^{im\theta + in\phi} \qquad (2)$$

Here Θ is the poloidal angle and r is the plasma minor radius. The electrostatic wave equation is $\nabla\cdot\overline{\overline{\varepsilon}}\cdot\nabla\Phi = 0$, where $\overline{\overline{\varepsilon}} = \hat{x}\hat{x}\varepsilon_{xx} + \hat{z}\hat{z}\varepsilon_{zz}$. We can expand this equation in the expansion parameter $\varepsilon = r/R_0$, where R_0 is the plasma major radius. Noting that, if we take the flux surfaces to correspond to constant r, we obtain

$$\varepsilon_{xx} = \varepsilon_{xxo} + \omega_{pe}^2/\omega_{ceo}^2\ (\varepsilon^2\cos^2\Theta + 2\varepsilon\cos\Theta) \tag{3a}$$

$$1/R \cong 1/R_0\ (1 - \varepsilon\cos\Theta + ...) \tag{3b}$$

where $\varepsilon_{xxo} = 1 + \omega_{pe}^2/\omega_{ceo}^2 - \omega_{pi}^2/\omega^2$, and ω_{ceo} is the electron cyclotron frequency at the plasma center. The wave equation then becomes

$$r^2\varepsilon_{xxo}\frac{\partial^2\Phi_m}{\partial r^2} + r\left(\frac{\partial}{\partial r}(r\varepsilon_{xxo})\right)\frac{\partial\Phi_m}{\partial r} + K_{mn}\Phi_m \tag{4}$$

$$= -\varepsilon F_1(\Phi_{m-1},\Phi_{m+1}) + \varepsilon^2 F_2 + ...$$

where

$$K_{mn}(r) = -m^2(\varepsilon_{xxo}\cos^2\delta + \varepsilon_{ZZ}\sin^2\delta) - 2k_\phi rm(\varepsilon_{ZZ} - \varepsilon_{xxo})\cos\delta\sin\delta - k_\phi^2 r^2(\varepsilon_{ZZ}\cos^2\delta + \varepsilon_{xxo}\sin^2\delta) \tag{5}$$

Here $\varepsilon_{ZZ} = 1 - \omega_{pe}^2/\omega^2$ and $k_\phi = n/R_0$.

The left hand side of equation (4) is just the wave equation for a linear plasma column; the right hand side of equation (4) couples together waves having different m numbers due to toroidal effects. In this paper we consider the first order coupling term εF_1, where

$$F_1 (\Phi_{m-1}, \Phi_{m+1}) = F_-(\Phi_{m-1}) + F_+(\Phi_{m+1}) \tag{6}$$

and

$$\begin{aligned} F_{\mp} (\Phi_{m\mp1}) = \Bigg[& - \frac{\omega_{pe}^2}{\omega_{ceo}^2 \, \varepsilon_{xxo}} \quad K_{m\mp1,\, n} \\ & - k_\phi r \cos\delta \sin\delta \; \frac{\omega_{pe}^2}{\omega_{ceo}^2} (m \mp 1) \\ & \mp \frac{1}{2} (m \mp 1)\left(1 + \frac{3\omega_{pe}^2}{\omega_{ceo}^2} \cos^2\delta - \frac{\omega_{pi}^2}{\omega^2} - \frac{\omega_{pe}^2}{\omega^2} \sin^2\delta\right) \\ & - \frac{\omega_{pe}^2}{\omega_{ceo}^2} \cos^2\delta (m \mp 1)^2 + k_\phi^2 r^2 \left(1 - \cos^2\delta \frac{\omega_{pe}^2}{\omega^2}\right) \\ & \pm k_\phi r \cos\delta \sin\delta \; \frac{\omega_{pe}^2}{\omega_{ceo}^2} \Bigg] \quad \Phi_{m\mp1} \\ & + \left[\frac{r^2}{\varepsilon_{xxo}} \frac{\partial}{\partial r} \left(\frac{\omega_{pe}^2}{\omega_{ceo}^2} \right) + \frac{r}{2} \left(1 + 3 \frac{\omega_{pe}^2}{\omega_{ceo}^2} - \frac{\omega_{pi}^2}{\omega^2}\right) \right] \frac{\partial \Phi_{m\pm1}}{\partial r} \end{aligned} \tag{7}$$

For small ε, F_1 will dominate the poloidal mode coupling.

Equation (4) has been solved on a VAX 11/780 computer using a Runge-Kutta integration scheme; the integration is started at the plasma edge with boundary conditions on Φ_m and Φ_m that correspond to an inward wave. Figure 1a plots the resulting $|\Phi(r,\theta)|$ over the plasma poloidal cross section for conditions similar to those of Alcator C. Here R_0 is taken as 100 cm so as to illustrate the full wave method, while still maintaining ε small. The edge boundary conditions are those for a uniform source at r = a = 16.5 cm that is 23 cm high, or that corresponds to a source centered on the outer midplane of the plasma having a poloidal extent of $\pm 46°$. Figure 1b plots the evolution of E(m), where

$$E(m) \equiv |\Phi(r)| \sqrt{k_r r\ \varepsilon_{xxo}} \qquad (8)$$

and $k_r = (K_{mn}/r^2\ \varepsilon_{xxo})^{1/2}$. For a plasma having no dissipation and $\varepsilon = 0$, E(m) would not change as r varies; $E(m)^2$ would then correspond to the wave power flux in mode m at a given r. $E(m)^2$ is here used to define the mean value of m, $\langle m \rangle$, and the variance in m, Δm. From figure 1b we see that E(m) greatly changes shape as the wave propagates inward from the launching structure. Figure 1b illustrates the importance of taking into account the finite poloidal size of the wave launcher in calculating lower hybrid wave propagation.

Figure 2a plots $|\Phi(r,\theta)|$ over the plasma cross section for the same parameters as those of figure 1, except that here the launcher height is reduced from 23 cm to 6 cm. The lower hybrid wave propagates into the plasma as a well defined cone, as might be expected from an $\varepsilon = 0$ treatment.

Figure 2b plots E(m) vs. r for this same case. As can be seen, the dominant change in the poloidal mode number spectrum is a shift in its mean m value <m> during the wave's first pass into the plasma, with only a small broadening of Δm. This figure shows that most of the broadening of the E(m) of figure 1 could be obtained by ray tracing if several appropriately weighted rays were launched at different poloidal locations on the waveguide array. Of course, the full wave solution does this explicitly.

Figure 3 shows a comparison of the radial behavior of <m> of a lower hybrid wave calculated using the full wave approach, and that using electrostatic ray tracing. The full wave method employs the same 6 cm high waveguide launcher. As can be seen, both methods yield similar results, illustrating that the full wave solution predicts the basic behavior of the ray tracing calculation. Some of the differences between the geometric optics and full wave solutions at high $\bar{n}_e$ are due to the ε expansion of the full wave solution which is not used for the ray tracing calculation.

Finally, the previous solutions did not consider the turning point behavior of the wave near r=0. This can be done by noting that for $r \ll a$ (and $\varepsilon \ll 1$) equation (4) becomes

$$r^2\Phi_m'' + r\Phi_m' + (\alpha^2 r^2 - m^2)\Phi_m = 0 \qquad (9)$$

where

$$\alpha^2 = \frac{\omega_{pe}^2}{\omega^2} \; \frac{(k_\phi + \frac{m}{R_o q_o})^2}{\varepsilon_{xxo}} \qquad (10)$$

and where q_o is the value of q at r=0.

The solution to equation (9) near r=0 is $\Phi_m(r) = CJ_m(\alpha r)$, where $J_m(X)$ is the Bessel function of the first kind of order m. Using this $\Phi_m(r)$ as a solution at small $r \approx m/\alpha$ near the wave turning point, we can numerically connect the incoming and outgoing lower hybrid waves at the plasma core and generate the $\Phi(r,\theta)$ that corresponds a complete pass of the wave through the plasma column. Figure 4a shows the resulting $|\Phi(r,\theta)|$ for the same plasma parameters as in figure 2. Figure 4b plots the evolution of $\langle m \rangle$ for this wave both on its inward and outward passes. Besides exhibiting the expected wave behavior, figure 4 illustrates this method of handling multiple passes of the plasma column. The wave trajectory could be further continued by connecting the incident and reflected waves at subsequent turning points.

Equation (4) can be straightforwardly generalized to handle higher orders of ε in mode coupling. In addition, the plasma thermal dispersion and the mode conversion to the hot ion mode can be included by incorporating the appropriate 4^{th} order derivative term into the left hand side of equation (4). The full electromagnetic lower hybrid wave equation could be formulated in a manner similar to equation (4), but its form would be more complex. In any case, such a modified equation (4) would explicitly calculate the distortion or broadening of the wave's m spectrum over long wave trajectories.

In summary, this paper presents a full wave treatment of lower hybrid wave propagation in toroidal plasmas. This technique should prove valuable in calculating lower hybrid wave evolution over long wave trajectories.

The author is happy to acknowledge the helpful suggestions of P. Bonoli, B. Lloyd, and Y. Takase concerning this work. This work was supported by U. S. Department of Energy Contract Number DE-AC02-78ET51013.

References

1. T. Yamamoto, et al., Phys. Rev. Lett. 45, 716 (1980).

2. T. Maekaewa, et al., Phys. Lett. 85A, 339 (1981).

3. S. C. Luckhardt, et al., Phys. Rev. Lett. 48, 152 (1982).

4. K. Ohkubo, et al., Nucl. Fusion 22, 203 (1982).

5. S. Bernabei, C. Daughney, P. Efthimion, et al., Phys. Rev. Lett. 49, 1255 (1982).

6. M. Porkolab, J. J. Schuss, Y. Takase, et al., in Proceedings of the 9th International Conference on Plasma Physics and Controlled Nuclear Fusion Research, Baltimore, U.S.A., 1982, Paper IAEA-CN-41/C-4.

7. J. J. Schuss, Bull. Am. Phys. Soc. 27, 962 (1982).

8. F. Jobes, J. Stevens, R. Bell, et al., Phys. Rev. Lett. 52, 1005 (1984).

9. P. T. Bonoli, E. Ott, Phys. Fluids 25, 359 (1982).

10. D. W. Ignat, Phys. Fluids 24, 1110 (1981).

11. Alan H. Glasser, Report PR3, Auburn University (Feb., 1980).

12. T. T. Lee, Z. G. An, Y. C. Lee, Bull. Am. Phys. Soc. 27, 1104 (1982).

Figure Captions

Fig. 1 a) $|\Phi(r,\theta)|$ plotted over the plasma column cross section for a lower hybrid wave launched by a 23 cm high waveguide at r = a = 16.5 cm. Here $n_\phi = (n/R_o)(c/\omega) = 3$, $R_o = 100$ cm, $B_{\phi o} = 100$ kG, f = 4.6 GHz, $\bar{n}_e = 10^{14}$ cm^{-3} and I_p = 400 kA in a deuterium plasma. Z points in the direction of the center line of the torus.

b) E(m) vs. r for the conditions of (a). Here at r = 5 cm, m has increased from 3 to 22 as <m> has changed by a comparable amount to -25.

Fig. 2 a) $|\Phi(r,\theta)|$ plotted over the plasma column cross section for a lower hybrid wave launched by a 6 cm high waveguide at r = 16.5 cm = a. Here $n_\phi = 3$, $R_o = 100$ cm, $B_{\phi o} = 100$ kG, f = 4.6 GHz, $\bar{n}_e = 10^{14}$ cm^{-3} and $I_p = 400$ kA in a deuterium plasma.

b) E(m) vs. r for the conditions of (a). At r = 3 cm <m> has decreased to -34 as Δm has only increased to 9 from a starting value of 7.

Fig. 3 Comparison of ray tracing (electrostatic) vs. full wave calculations of <m> for a lower hybrid wave launched by a 6 cm high waveguide at r=a. Here we choose $\bar{n}_e = 2 \times 10^{14}$ cm^{-3}, 1×10^{14} cm^{-3} and 3×10^{13} cm^{-3}, and we fix $R_o = 100$ cm, a = 16.5 cm, $B_{\phi o} = 100$ kG, f = 4.6 GHz, $I_p = 400$ kA in a deuterium plasma. (RT = ray tracing, W = full wave).

Fig. 4 a) $|\Phi(r,\theta)|$ plotted over the plasma cross section for the conditions of figure 2, except that here the lower hybrid

wave enters and exits the plasma core and is followed until it reaches the plasma boundary.

b) <m> vs. r for both the inward and outward propagating waves.

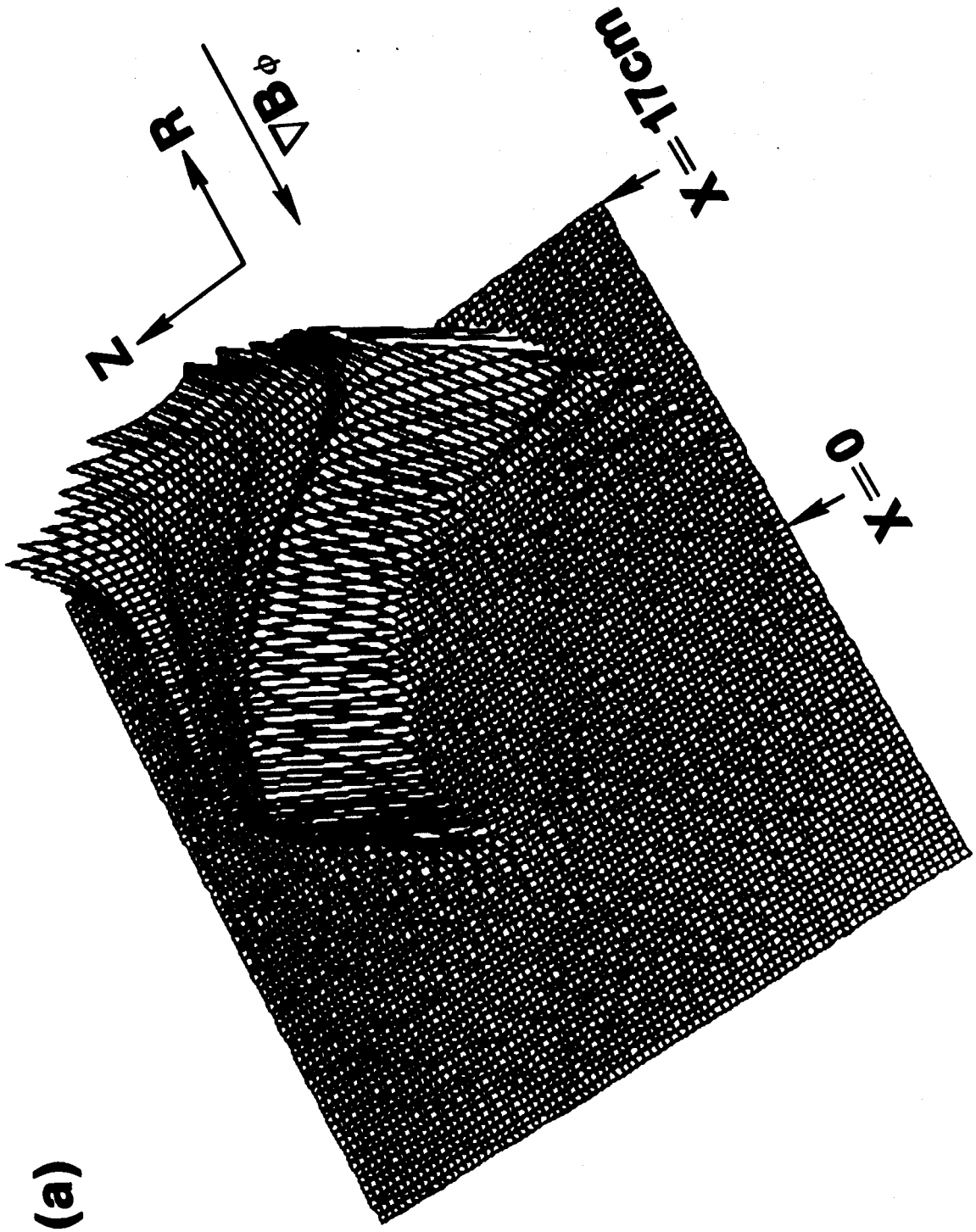

FIGURE 1a

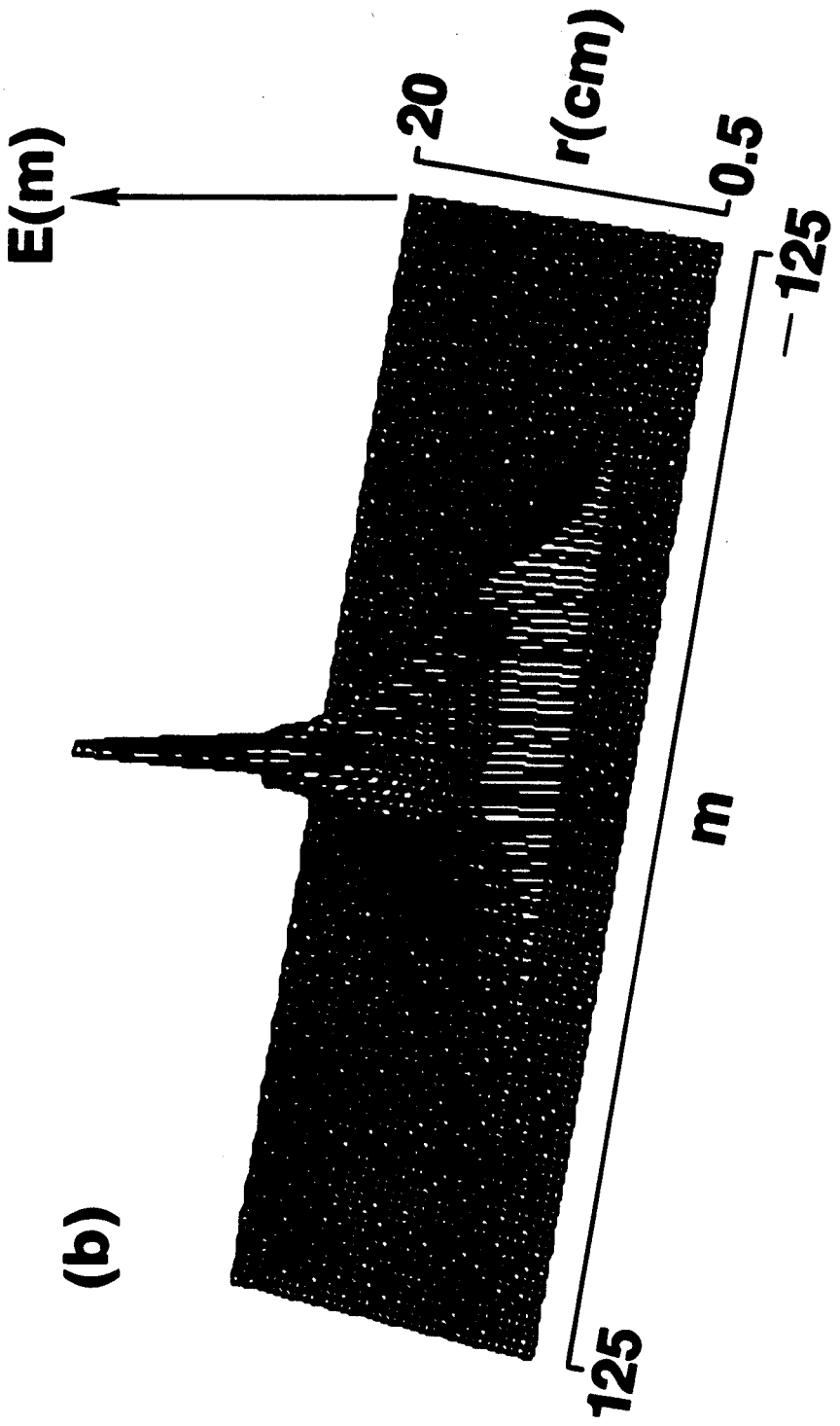

FIGURE 1b

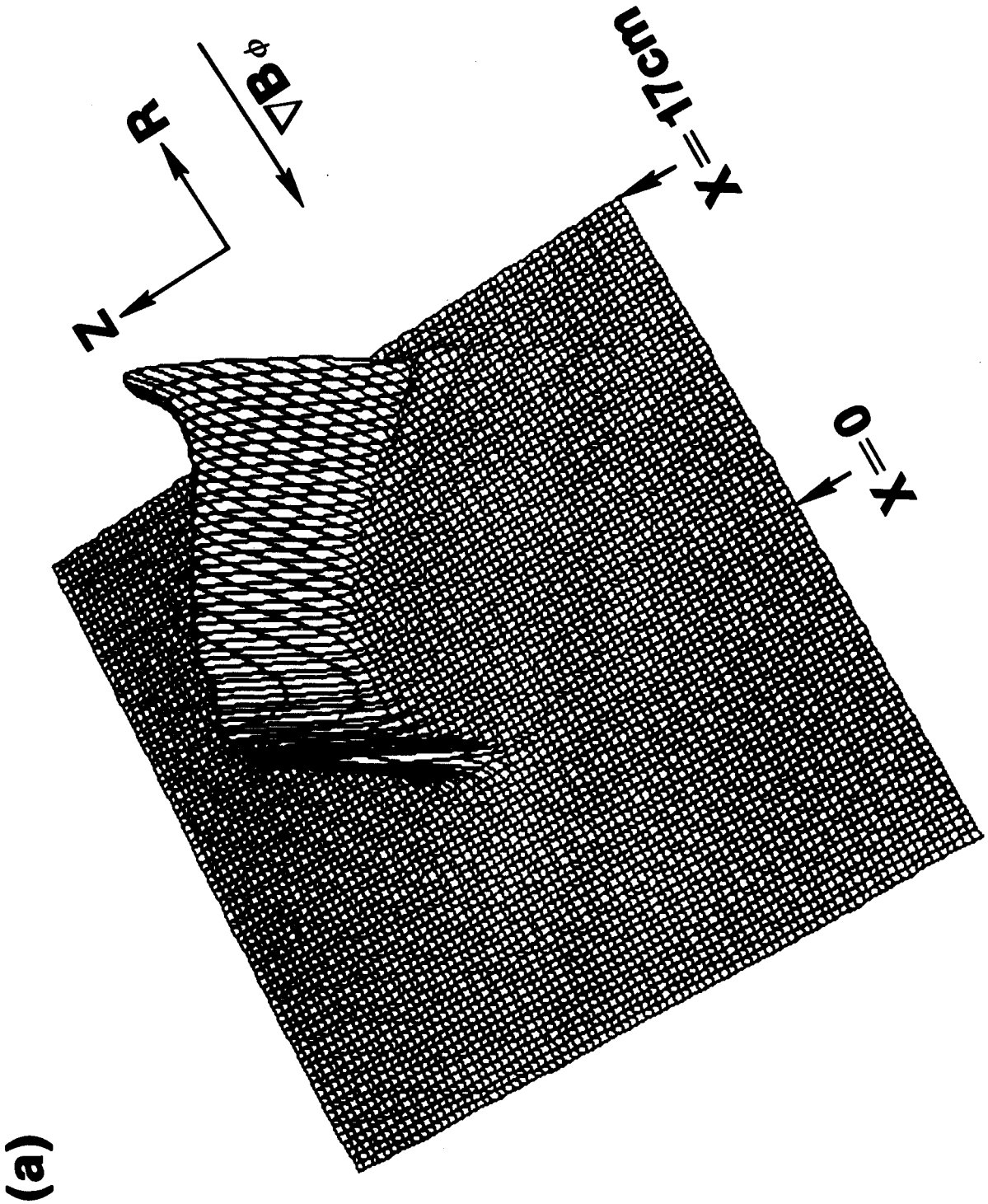

FIGURE 2a

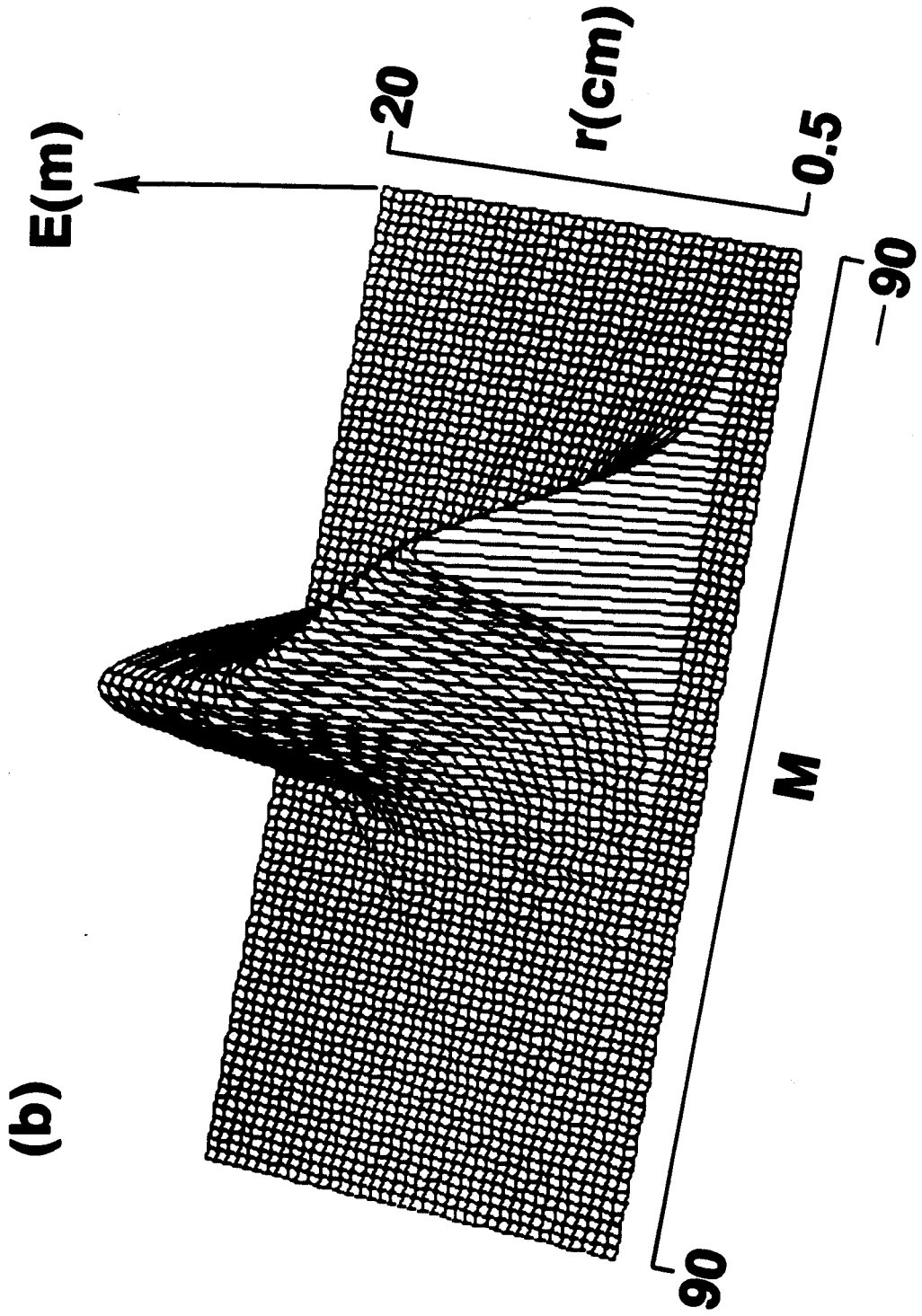

FIGURE 2b

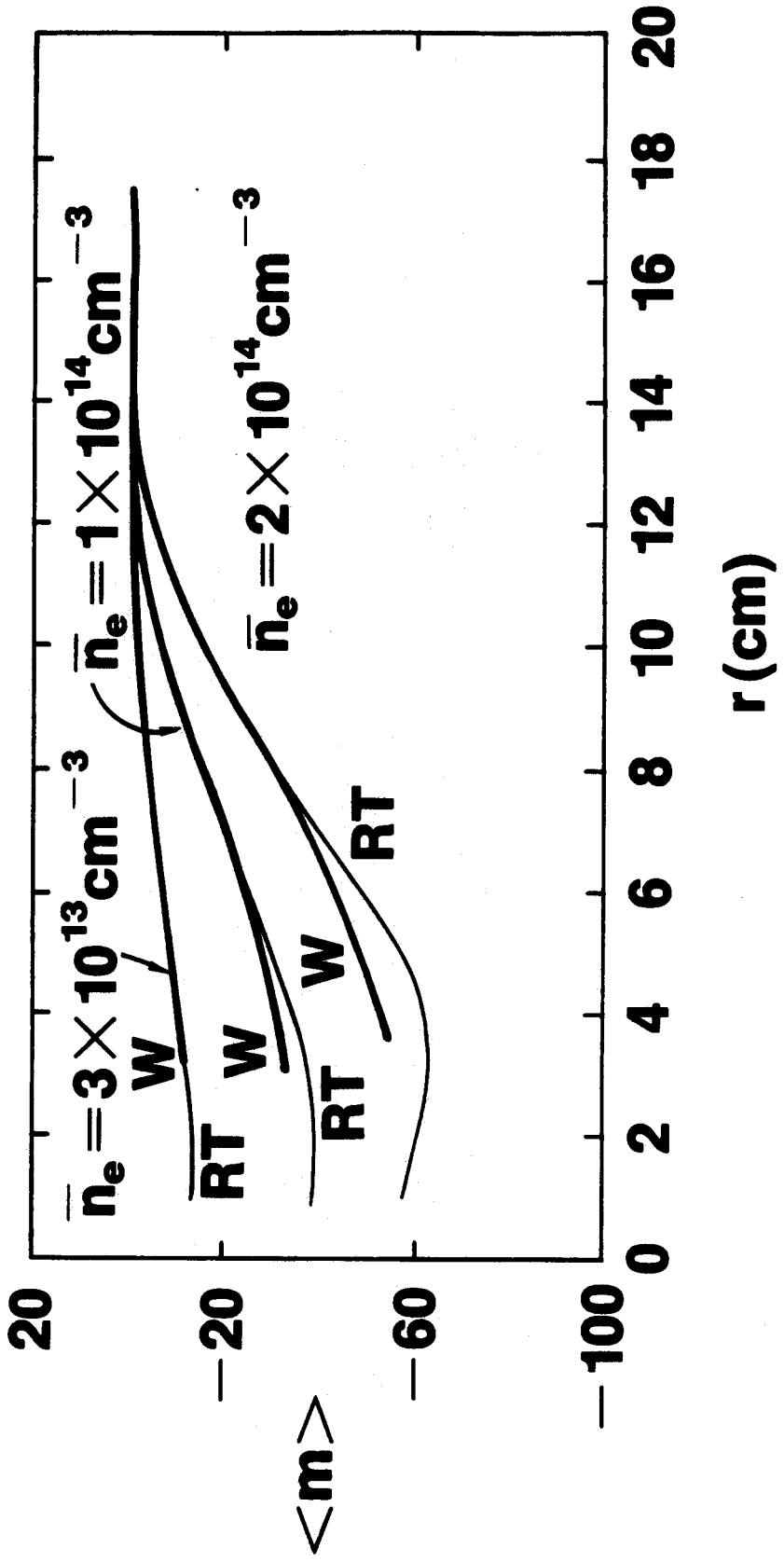
$\bar{n}_e = 3 \times 10^{13} cm^{-3}$
$\bar{n}_e = 1 \times 10^{14} cm^{-3}$
$\bar{n}_e = 2 \times 10^{14} cm^{-3}$
W
RT
W
RT
W
RT
20
−20
−60
−100
0
2
4
6
8
10
12
14
16
18
20
r(cm)
⟨m⟩

FIGURE 3

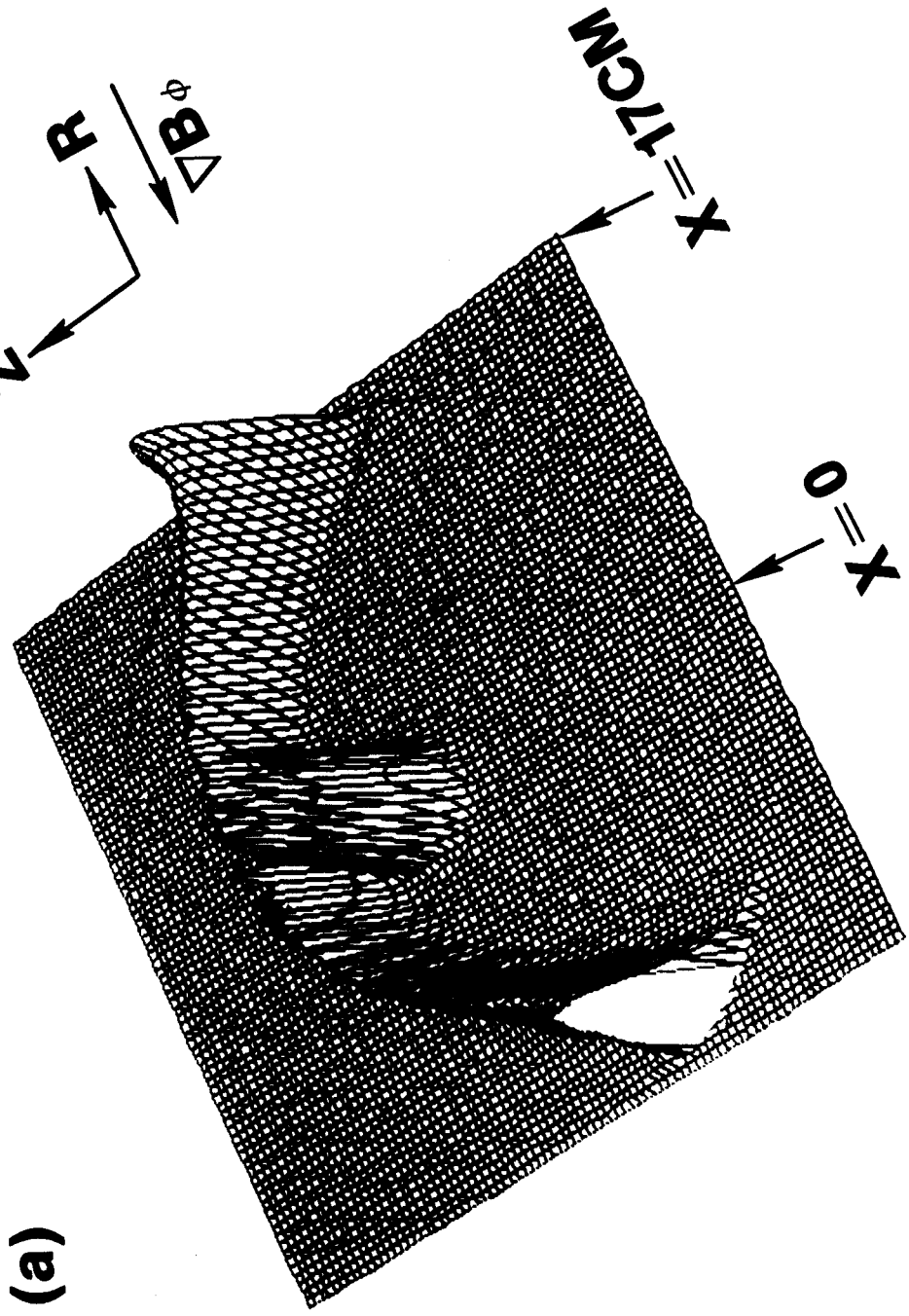

FIGURE 4a

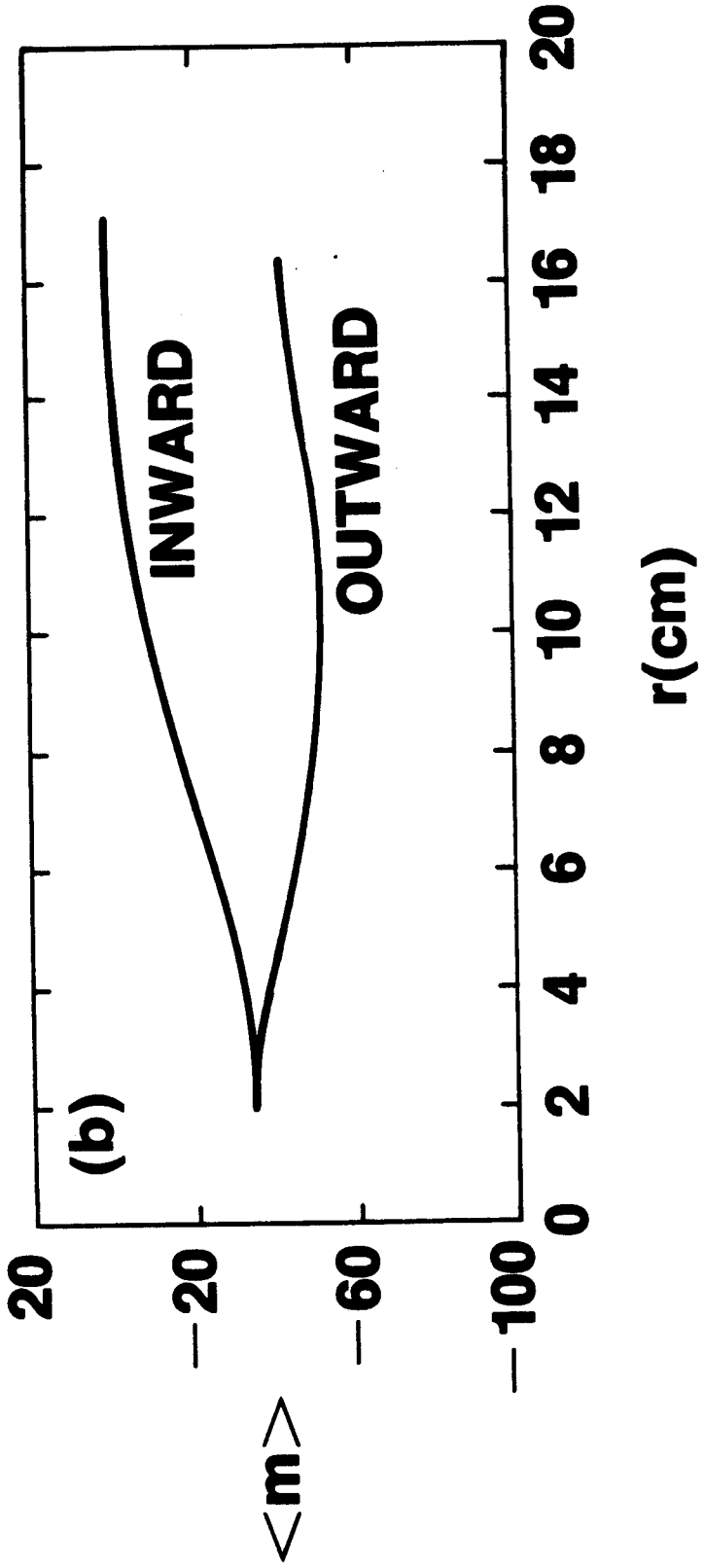

FIGURE 4b